



## Vortex features and vortex-induced vibration behavior under varying flow conditions

Yun-Jae Kim<sup>1</sup> · Sung-Woong Choi<sup>†</sup>

(Received January 8, 2026 : Revised January 21, 2026 : Accepted January 25, 2026)

**Abstract:** Vortex-induced vibration (VIV) is a critical factor that governs the fatigue performance and long-term structural integrity of submarine power cables exposed to ocean currents. As offshore energy infrastructure continues to expand into deeper waters and more dynamic marine environments, a reliable understanding of vortex shedding characteristics and the associated VIV behavior under realistic tidal conditions has become increasingly important. In this study, a numerical investigation was conducted to analyze the vortex features and VIV behavior of structures subjected to varying flow conditions. The numerical methodology was validated through benchmark simulations of a steady flow past a circular cylinder at a Reynolds number of 40. The key vortex characteristics, including the recirculation zone length, vortex center locations, separation angle, and drag coefficient, were quantitatively compared with reference experimental and numerical data reported in the literature. Furthermore, the lift and drag coefficients, vortex shedding characteristics, and Strouhal frequencies were systematically evaluated over a range of Reynolds numbers. The results demonstrated that the proposed numerical approach accurately captures the essential hydrodynamic features governing vortex shedding and provides reliable predictions of VIV-related flow responses.

**Keywords:** Vortex-induced vibration, Vortex shedding, Reynolds number, Numerical analysis

### 1. Introduction

Submarine power cables play a critical role in offshore engineering systems, particularly offshore wind farms, subsea power transmission networks, and marine renewable energy infrastructures. As the offshore wind capacity continues to expand toward deeper waters and harsher marine environments, submarine cables are increasingly subjected to complex hydrodynamic loading conditions. Among these, vortex-induced vibration (VIV) has been recognized as one of the dominant mechanisms responsible for the fatigue damage and long-term structural degradation of slender cylindrical structures installed in marine environments [1].

VIV occurs when alternating vortices are shed from the surface of a structure exposed to crossflow, generating periodic lift forces that induce oscillatory motions. For submarine cables resting on or spanning above the seabed, such flow-induced oscillations may be triggered by steady currents, tidal flows, or combined wave-current interactions. When the vortex shedding frequency

approaches the natural frequency of a cable, a lock-in phenomenon occurs, leading to large vibration amplitudes and accelerated fatigue accumulation [2]. Vortex shedding is generally initiated when a stable pair of vortices becomes unstable under small disturbances; this phenomenon typically appears at Reynolds numbers ( $Re$ ) greater than 40. Beyond this threshold, the flow field surrounding the structure becomes unstable, resulting in alternating vortex formations and periodic hydrodynamic forces acting on the structure [3]. Owing to its fundamental nature, the laminar flow regime at  $Re \approx 40$  has been widely adopted as a benchmark for validating numerical methods for vortex shedding and VIV analysis.

Extensive studies have been conducted to investigate the vortex features and their associated flow characteristics. Linnick and Fasel [4], Herfjord [5], and Berthelsen and Faltinsen [6] systematically analyzed vortex shedding behavior in low-Reynolds-number flows, focusing on parameters such as the drag coefficient ( $C_d$ ), recirculation zone length ( $L/D$ ), vortex center

<sup>†</sup> Corresponding Author (ORCID: <http://orcid.org/0000-0001-7285-4257>): Assistant Professor, Department of Mechanical System Engineering, Gyeongsang National University, (53064) 2, Tongyeonghaean-ro, Tongyeong-si, Gyeongsangnam-do, Republic of Korea, E-mail: [younhulje@gnu.ac.kr](mailto:younhulje@gnu.ac.kr), Tel: 055-772-9103

<sup>1</sup> M. S., Department of Mechanical System Engineering, Gyeongsang National University, E-mail: [dbswoznemtm@gnu.ac.kr](mailto:dbswoznemtm@gnu.ac.kr), Tel: 055-772-9103

This is an Open Access article distributed under the terms of the Creative Commons Attribution Non-Commercial License (<http://creativecommons.org/licenses/by-nc/3.0>), which permits unrestricted non-commercial use, distribution, and reproduction in any medium, provided the original work is properly cited.

locations ( $a/D$ ,  $b/D$ ), and separation angle ( $\theta$ ). Further investigations by Russell and Wang [7], Xu and Wang [8], and Calhoun [9] examined the influence of wake structure and separation characteristics on the VIV behavior, providing fundamental insights into flow-induced vibration mechanisms.

Despite these advances, studies on the vortex-induced vibration (VIV) behavior of structures under a wide range of flow conditions remain limited. Therefore, this study aims to numerically investigate the vortex features and VIV behavior of a structure subjected to varying flow conditions. Emphasis was placed on validating the adopted numerical methodology through benchmark comparisons of vortex characteristics, followed by the application of the validated model to evaluate the dynamic response of the structure under representative fluid flow conditions.

## 2. Theory

### 2.1 Vortex Shedding

Vortex-induced vibration (VIV) is a critical issue in the design and operation of slender offshore structures such as risers, umbilicals, and submarine power cables because periodic vortex shedding can generate cyclic hydrodynamic forces that lead to fatigue damage. When an external flow exceeds a critical velocity, flow separation occurs because of the strong adverse pressure gradient on the downstream side of the structure, resulting in the formation of alternating vortices. The interaction between these unsteady vortices and the structural motion induces oscillatory responses, commonly referred to as VIV [10].

Submarine power cables are continuously exposed to complex marine environments throughout their service life and are subjected to combined external excitations resulting from ocean waves and currents. Steady or slowly varying tidal currents, together with the excitation transmitted from floating platforms or upper supporting structures, can trigger vortex shedding and subsequently induce VIV. Such flow-induced vibrations are widely recognized as some of the dominant mechanisms responsible for fatigue accumulation and long-term structural degradation in submarine cable systems. Vortex shedding occurs at a characteristic frequency, known as the vortex shedding frequency  $f_s$ , which is primarily governed by the incoming flow velocity  $U$  and characteristic diameter of the structure  $D$ . This frequency is commonly expressed in a dimensionless form using the Strouhal number ( $S_t$ ), which is defined as

$$S_t = \frac{f_s D}{U} \quad (1)$$

The Strouhal number provides a fundamental relationship linking the flow conditions to the frequency of the unsteady hydrodynamic loading acting on slender marine structures.

### 2.2 Reynolds Number Dependent Vortex Shedding

The Strouhal number is closely related to  $Re$  and remains approximately constant within specific  $Re$  ranges, whereas it gradually varies as the wake structure and turbulence characteristics evolve with increasing  $Re$ . At relatively low  $Re$  values, laminar vortex shedding develops in the wake of the circular cylinder, producing highly regular and periodic fluid-force fluctuations. Vortex shedding is typically initiated when a pair of initially stable vortices becomes unstable under small disturbances, which occurs at  $Re$  values greater than 40. In this regime, the boundary layer formed on the surface of the cylinder separates owing to an adverse pressure gradient on the rear side, resulting in alternating vortex formation in the wake. Under low-current conditions,  $Re$  generally falls within the range of 40–200, which corresponds to laminar wake flow regimes. As  $Re$  increases toward  $\approx 1000$ , the wake flow enters a transitional regime, where the vortex street gradually evolves from laminar to turbulent behavior. In this range, vortices tend to form closer to the cylinder surface, and both the shedding frequency and amplitude characteristics are modified. When  $Re > 1000$ , the wake region behind the cylinder becomes fully turbulent, significantly altering the vortex shedding patterns and the associated unsteady hydrodynamic forces.

These Reynolds-number-dependent changes in wake dynamics directly affect the magnitude and frequency of the fluid forces acting on the structure, thereby affecting the vibration amplitude, response mode, and frequency-lock-in behavior associated with VIV. Consequently, a systematic understanding of vortex shedding mechanisms across different  $Re$  regimes is essential to accurately predicting VIV responses and assessing fatigue damage in submarine cable systems subjected to tidal current loading.

## 2. Numerical Analysis

### 2.1 Numerical Conditions

A VIV analysis of a structure was performed to investigate the influence of various fluid conditions. The characteristic vortex features and hydrodynamic parameters were examined to validate the numerical methodology. In this context, as shown in **Figure 1**,  $D$  denotes the diameter of the cylindrical structure, whereas  $L$ ,  $a$ , and  $b$  represent characteristic geometric lengths associated with the wake structure, and  $\theta$  denotes the vortex separation angle. These parameters enabled quantitative evaluation of

**Table 1:** Vortices features measurements of a steady flow past a circular cylinder for  $Re=40$

Experiments	Re = 40				
	L/D	a/D	b/D	(degree)	Cd
Linnick and Fasel [4]	2.28	0.27	0.60	53.6	1.54
Herfjord [5]	2.25	0.71	0.60	51.2	1.60
Berthelsen and Faltinsen [6]	2.29	0.72	0.60	53.9	1.59
Russel and Wang [7]	2.29	-	-	53.1	1.60
Xu and Wang [8]	2.21	-	-	53.5	1.66
Calhoun [9]	2.18	-	-	54.2	1.62
Average	2.25	0.72	0.60	53.3	1.60
Validation study	2.35	0.70	0.65	53.0	1.61
Deviation (%)	4.44	2.33	8.33	0.47	0.52

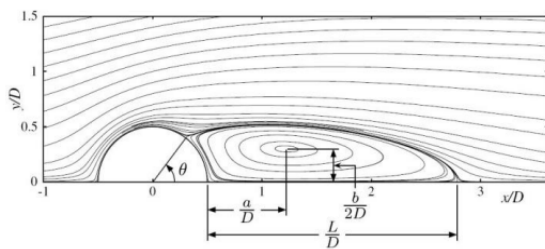


**Figure 1:** Vortex features for  $Re=40$

vortex characteristics, including the normalized  $L/D$  and  $a/D$  and  $b/D$ . The numerical predictions were systematically compared with benchmark data reported in the literature to verify the reliability and accuracy of the adopted analytical approach.

Numerical simulations were performed using the commercial computational fluid dynamics software ANSYS Fluent (2024 R2). An unsteady flow analysis was performed, and pressure–velocity coupling was handled using the pressure-implicit with splitting of operators algorithm to ensure numerical stability and accuracy in the transient simulations [11]. The shear stress transport ( $k-\omega$  SST) turbulence model was employed, as it provides reliable predictions of flow separation and wake development, which are essential for accurately capturing vortex shedding behavior and VIV characteristics.

### 3. Results

#### 3.1 Validation of Numerical Method

To validate the developed numerical approach for VIV analysis, we quantitatively compared the calculated vortex features with reference data reported in previous experimental and numerical studies for steady flow past a circular cylinder at  $Re = 40$ . The validity of the proposed methodology was assessed by examining the agreement between the present numerical results and the established benchmark values.

The vortex feature results obtained using the proposed

numerical approach are shown in **Figure 2**. Key geometric and hydrodynamic parameters characterizing the vortex structures were employed as validation metrics, including the normalized  $L/D$ ,  $a/D$  and  $b/D$ ,  $\theta$ , and  $Cd$ . The predicted  $L/D$  was 2.35, which corresponded to a deviation of approximately 4.44% from the average reference value of 2.25, indicating that the wake extent behind the cylinder was accurately captured.

The vortex center locations exhibited deviations of approximately 2.33% for  $a/D$  and 8.33% for  $b/D$ . Although a relatively large deviation was observed for  $b/D$ , the overall symmetry and spatial distribution of the vortex structures remained consistent with the reference studies. The separation angle was predicted to be  $53.0^\circ$ , showing an error of only 0.47% compared with the average reference value of  $53.25^\circ$ , demonstrating that the vortex detachment behavior was reliably reproduced.

Furthermore, the predicted drag coefficient ( $Cd = 1.61$ ) exhibited a relative error of approximately 0.52% compared with the reference mean value of 1.60, confirming that the integrated hydrodynamic response was accurately captured. As illustrated in **Figure 2**, identical vortices were clearly observed in the wake region behind the cylindrical surface. A quantitative comparison of the vortex features is presented in **Table 1**. Overall, the strong

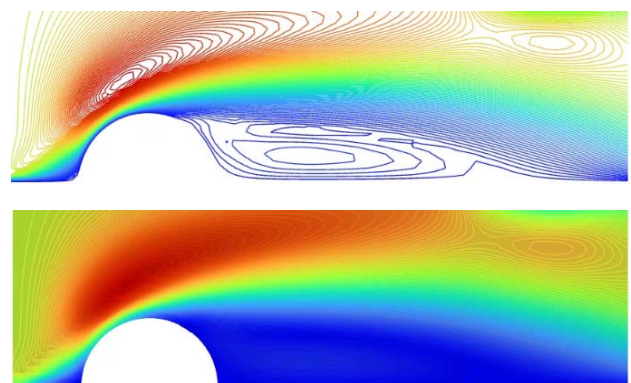


**Figure 2:** Vortex feature results obtained using the developed numerical approach

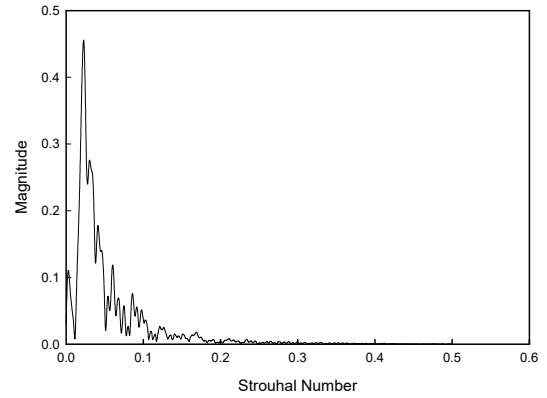
agreement between the present numerical results and benchmark data demonstrates the validity and robustness of the developed numerical method for VIV analysis.

### 3.2 Evaluation of Lift and Drag Coefficients with Respect to Re

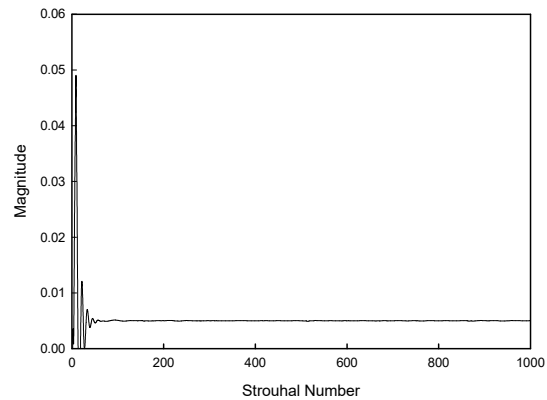
Figure 3 illustrates the time histories of the lift coefficient (CL), Cd, and the corresponding Strouhal frequency obtained from the transient laminar flow simulations at Re = 40 and 100. **Table 2** presents a quantitative comparison of the Cd and CL values at Re = 100 and 200 between the present numerical results and representative experimental and numerical data reported in the literature.

At Re = 40, the flow remained in a stable laminar regime characterized by the formation of symmetric and attached recirculation vortices behind the cylinder. Under these conditions, the drag coefficient converged to a nearly constant value after the initial transient period, whereas the lift coefficient exhibits small-amplitude oscillations near zero. The Strouhal spectrum exhibited a distinct dominant peak, indicating a well-defined vortex-shedding frequency associated with laminar vortex shedding. As Re increased to 100 and 200, the periodic vortex shedding became more pronounced, leading to a clearer oscillatory behavior in the lift coefficient time history. The drag coefficient maintained a relatively stable mean value with small superimposed fluctuations, reflecting a balance between the viscous and inertial effects in the laminar wake regime. The Strouhal number extracted from the frequency analysis remained within the range reported in previous studies, confirming that the dominant shedding frequency is appropriately captured using the present numerical approach.

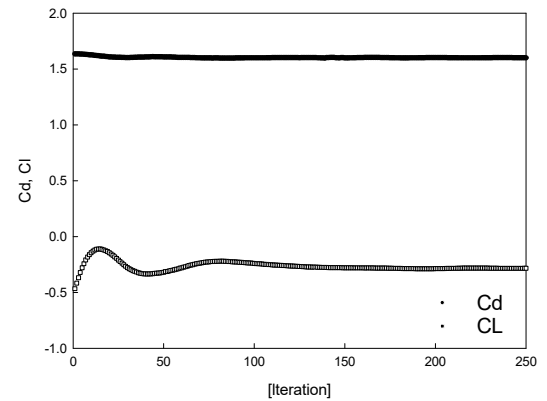
A detailed quantitative comparison with the reference data is presented in **Table 2**. For Re = 100, the average drag coefficient reported in the literature is  $C_d \approx 1.35$ , whereas the present numerical result yields  $C_d = 1.19$ , corresponding to a deviation of approximately 11.9%. For Re = 200, the average reference value is  $C_d \approx 1.31$ , whereas the present result is  $C_d = 1.12$ , resulting in a deviation of about 14.5%. Although the present simulations systematically underestimated the drag coefficient, the predicted values remained within the scatter range of the experimental and numerical results reported in the literature. With respect to the lift coefficient, the average reference value at Re = 200 is  $CL \approx 0.59$ , while the present numerical result gives  $CL = 0.51$ , corresponding to a deviation of approximately 13.6%. Considering the sensitivity of the lift force prediction to the mesh resolution, numerical



(a)



(b)



(c)

**Figure 3:** Strouhal frequency with laminar flow of different at Reynolds numbers of Re = 40 and 100, the lift coefficient (CL), drag coefficient (Cd) with Strouhal frequency (a: Re=40, b: Re=100, c: Re=200)

scheme, and flow unsteadiness, this level of discrepancy is considered acceptable. Importantly, the proposed model successfully reproduces the overall magnitude and oscillatory nature of the lift coefficient associated with vortex shedding.

Overall, the comparisons of the Cd, CL, and Strouhal frequencies demonstrate that the present numerical method captures the

**Table 2:** Quantitative comparison of Cd and CL values at Re = 100 and 200

Experiments	Re = 100	Re = 200	
	Cd	Cd	Cl
Linnick and Fasel [4]	1.34	1.34	0.69
Herfjord [5]	1.36	1.35	0.7
Berthelsen and Faltinsen [6]	1.38	1.37	0.7
Russel and Wang [7]	1.38	1.29	0.5
Xu and Wang [8]	1.42	1.42	0.66
Calhoun [9]	1.33	1.17	0.67
Franke, <i>et al.</i> [12]	-	1.31	0.65
Rajani, <i>et al.</i> [13]	1.34	1.34	0.42
Asyikin [14]	1.28	1.2	0.29
Average	1.35	1.31	0.59
Validation study	1.19	1.12	0.51
Deviation (%)	11.9	14.5	13.6

essential hydrodynamic characteristics of the flow past a circular cylinder over a range of Re. The observed deviations from the reference data are within reasonable bounds and are consistent with the differences reported in previous studies. Therefore, the developed numerical approach is deemed sufficiently accurate and reliable for subsequent VIV analyses of submarine cable structures under current-induced loading conditions.

#### 4. Conclusion

In this study, a numerical framework was developed and validated to investigate the vortex features and vortex-induced vibration (VIV) behavior of a structure under varying flow conditions. Validation against benchmark data for steady flow past a circular cylinder at Re = 40 showed strong agreement, with deviations of approximately 4.44% for the recirculation zone length, 2.33% and 8.33% for vortex center locations, 0.47% for the separation angle, and 0.52% for the drag coefficient, confirming the reliability of the numerical methodology.

Parametric analyses over Reynolds numbers of 40–200 demonstrated that the proposed model accurately captures the evolution of the lift and drag coefficients and the associated vortex shedding frequencies. Although an underestimation of the drag and lift coefficients was observed at higher Reynolds numbers, the predicted values remained within the scatter range reported in previous experimental and numerical studies.

Overall, the developed numerical approach successfully reproduces the key hydrodynamic characteristics governing vortex shedding and VIV behavior and is considered sufficiently accurate for subsequent analyses of submarine cable vibration responses under realistic tidal current conditions. These results provide a robust basis for future fatigue assessments and design

optimization of submarine cable systems in offshore environments.

#### Acknowledgement

This work was supported by the Korea Institute of Energy Technology Evaluation and Planning (KETEP) grant funded by the Korea government (MOTIE) (20213000000020, Development of core equipment and evaluation technology for construction of subsea power grid for offshore wind farm).

#### Author Contributions

Conceptualization, Y. J. Kim, S. W. Choi; Methodology, Y. J. Kim, S. W. Choi; Software, Y. J. Kim, S. W. Choi; Formal Analysis, Y. J. Kim, S. W. Choi; Investigation, Y. J. Kim, S. W. Choi; Resources, S. W. Choi; Data Curation S. W. Choi; Writing-Original Draft Preparation, S. W. Choi; Writing-Review & Editing, S. W. Choi; Visualization, Y. J. Kim, S. W. Choi; Supervision, S. W. Choi; Project Administration, S. W. Choi.

#### References

- [1] A. K. Vo, T. L. Mai, H. K. Yoon, and S. H. Ahn, "Steady Towing Simulation of Underwater Hairy Fairing Cable System," *Journal of Ocean Engineering and Technology*, 2025
- [2] W. Lee and B. W. Nam, "Numerical analysis of wave interference effects on ship resistance in parallel arrangements," *Journal of Ocean Engineering and Technology*, vol. 38, no. 6, pp. 325–335, 2024.
- [3] H. Zhao, J. H. Jeon, D. I. Yu, and Y. W. Lee, "Effects of circular cylinder rotating ratios on wake vortex suppression

- using OpenFOAM,” *Journal of Advanced Marine Engineering and Technology*, vol. 49, no. 3, pp. 168–178, 2025.
- [4] M. N. Linnick and H. F. Fasel, “A high-order immersed interface method for simulating unsteady incompressible flows on irregular domains,” *Journal of Computational Physics*, vol. 204, no. 1, pp. 157–192, 2005.
- [5] K. Herfjord, A study of two-dimensional separated flow by a combination of the finite element method and Navier–Stokes equations, Dr. Ing. Thesis, Department of Marine Hydrodynamics, Norwegian Institute of Technology, Norway, 1996
- [6] P. A. Berthelsen and O. M. Faltinsen, “A local directional ghost cell approach for incompressible viscous flow problems with irregular boundaries,” *Journal of Computational Physics*, vol. 227, pp. 4354–4397, 2008.
- [7] D. Russell and Z. J. Wang, “A Cartesian grid method for modeling multiple moving objects in 2D incompressible viscous flow,” *Journal of Computational Physics*, vol. 191, no. 1, pp. 177–205, 2003.
- [8] S. Xu and Z. J. Wang, “An immersed interface method for simulating the interaction of a fluid with moving boundaries,” *Journal of Computational Physics*, vol. 216, no. 2, pp. 454–493, 2006.
- [9] D. Calhoun, “A Cartesian grid method for solving the two-dimensional streamfunction-vorticity equations in irregular regions,” *Journal of Computational Physics*, vol. 176, no. 2, pp. 231–275, 2002.
- [10] C. S. Sim, M. S. Kim, C. M. Kim, Y. H. Roh, J. B. Lee, K. S. Chae, K. Kim, and D. Jeong, “A Fundamental Study of VIV Fatigue Analysis Procedure for Dynamic Power Cables Subjected to Severely Sheared Currents,” *Journal of the Society of Naval Architects of Korea*, vol. 60, no. 5, 375–387, 2023 (in Korean).
- [11] J. H. Park, J. H. Jeon, and Y. W. Lee, “Study on fluid flow and flow-induced noise simulation for a circular cylinder,” *Journal of Advanced Marine Engineering and Technology*, vol. 49, no. 4, pp. 269–282, 2025.
- [12] R. Franke, W. Rodi, and B. Schonung, “Numerical calculation of laminar vortex shedding flow past cylinders,” *Journal of Wind Engineering and Industrial Aerodynamics*, vol. 35, pp. 237–257, 1990.
- [13] B. N. Rajani, A. Kandasamy, S. Majumdar, “Numerical simulation of laminar flow past a circular cylinder,” *Journal of Applied Mathematical Modelling*, vol. 33, pp. 1228–1247, 2009.
- [14] M. T. Asyikin, CFD Simulation of Vortex Induced Vibration of a Cylindrical Structure, M.S. Thesis, Department of Civil and Transport Engineering, Norwegian University of Science and Technology (NTNU), Norway, 2012.